Hierarchical Mixed-Domain Circuit Simulation, Synthesis and Extraction Methodology for MEMS

Tamal Mukherjee[†] and Gary K. Fedder[†*]

[†]Department of Electrical and Computer Engineering and [*]The Robotics Institute
Carnegie Mellon University
Pittsburgh, PA, 15213-3890

Abstract

Emerging results for mixed-domain circuit simulation, a component-level synthesis strategy, and a layout extractor is presented for use in design of microelectromechanical systems (MEMS). The mixed-domain circuit representation is based on Kirchhoffian network theory. Micromechanical and electromechanical components may be partitioned hierarchically into low-level reusable elements. The MEMS component-level synthesis approach uses optimization to generate microstructure layout that meets specified performance criteria. A feature-recognition based extractor for verification translates layout geometry into the mixed-domain circuit representation. A common MEMS component, the integrated microresonator, demonstrates the use of these tools. Lumped-parameter MEMS simulation of the resonant frequency matches finite-element analysis to 1 % and fabricated resonators match to within 4 % of the synthesized performance. Based on this initial work, a hierarchical structured design methodology for integrated microsystems that is compatible with standard VLSI design is proposed.

1. Introduction

Digital design tools such as logic synthesis, semicustom layout and behavioral simulation have drastically changed the digital IC design process, enabling design of complex "systems on a chip". The usefulness of such chips are limited in a world dominated by information that is not represented by 0s and 1s. Overcoming these limitations has led to *mixed-signal* and *mixed-domain*

1

technologies that monolithically integrate CMOS electronics with microelectromechanical systems (MEMS) leading to chips that can sense and actuate as well as compute.

MEMS are micron to millimeter sized systems integrating electrical and mechanical elements [1][2][3]. They are fabricated using microelectronic batch processing techniques and can sense, control and actuate on the micro scale. Moreover, arrays of MEMS devices can be used for macro scale sensing and actuation. Researchers are using MEMS in diverse application areas such as inertial navigation systems [4], digital mirror displays [5], DNA analysis systems [6], RF distributed sensor networks [7], and probe-based data storage systems [8]. These systems incorporate truly mixed technology, integrating combinations of digital and analog electronics, mechanical structures, electromechanical actuators, and fluidic chambers.

The advent of stable, VLSI-compatible MEMS fabrication technologies has led to the development of increasingly complex and integrated MEMS-based systems. Future systems are expected to contain hundreds or even thousands of mixed-domain devices. This has led to a desperate demand for CAD tools to support rapid design of systems involving physical interactions between mechanical, electrostatic, magnetic, thermal, fluidic, and optical domains. As in traditional electronic design, hierarchical design methodologies, mixed-domain circuit simulators, layout synthesis tools, and layout extraction will enable MEMS engineers to build larger systems and allow them to concentrate on system-level design issues.

The next section is a background section on MEMS technology, devices, and the current approach to designing MEMS. This is followed, in Section 3, by a description of the levels of abstraction in the MEMS design methodology. Each of the individual tools currently being developed to enable integrated electronics/MEMS design is described next; namely, simulation in Section 4, synthesis in Section 5 and extraction in Section 6. Included in each of the sections are

the results of using each of the tools on a MEMS design. A complete integrated electronics/MEMS design flow is proposed in Section 7. Finally, Section 8 offers some concluding remarks.

2. Background

2.1. MEMS Fabrication

Batch fabrication techniques, similar to VLSI electronics, are used to manufacture MEMS devices. Therefore, MEMS can exploit the same cost benefits that arise from such integration. There are three major technologies [1][2][9] used in MEMS fabrication: bulk micromachining, LIGA and surface micromachining. As in the VLSI world, silicon-based technologies tend to be the most widely used, both because silicon is a thoroughly studied material and its wide availability. In bulk micromachining the mechanical structures are etched out of the bulk of the silicon wafer whereas surface-micromachined structures are made from the thin-film layers deposited on the surface of the wafer. The LIGA (German acronym for LIthographie, Galvanoformung, Abformung) technique involves X-ray lithography, micro-electroplating and micro-molding processes, and is difficult to integrate with electronics.

Within the last decade, surface-micromachining techniques have exhibited phenomenal growth. Surface-micromachined devices are fabricated by deposition, patterning, and etching of thin films, a set of process steps commonly used for VLSI fabrication. Additionally, a release step is needed, to etch a sacrificial layer, thereby releasing the mechanical structure. A commonly used surface-micromachining process is the Multi-User MEMS Process service (MUMPS) from MCNC [10]. The need to electronically process the signals generated by MEMS sensors, and/or electronically control MEMS actuators has led to the development of integrated surface-micromachining processes. Currently, monolithically integrated MEMS fabrication alternatives in the U.S. include the Sandia Agile MEMS Prototyping, Layout tools, and Education program (SAMPLE) [11][12], and

3

the iMEMS^{TM} process [13], both of which use polysilicon as the structural material. An alternative to polysilicon microstructures are CMOS micromachining processes in which structures are made from CMOS dielectric and metal layers [14][15]. CMOS-MEMS processes decouple the micromachining steps from the CMOS process flow, leading to the advantages of low-cost fabrication of integrated MEMS, an ability to place multiple isolated conductors within suspended structures.

This paper focuses on polysilicon surface-micromachining process due to its simplicity, popularity, and maturity [16]. An example polysilicon MEMS layout is shown in Figure 1. The device consists of a floating structural layer that is attached to the substrate by anchors. Figure 2 details the fabrication process steps for such devices. In particular it shows the cross-section A-A' of Figure 1 at different points of the fabrication process. First a layer of low-stress silicon nitride is deposited on the substrate for electrical insulation. This is followed by deposition of a polysilicon layer, which is patterned and etched to form electrical interconnects. A sacrificial layer of phosphosilicate glass (PSG) is then deposited and patterned to form dimples and the first anchor holes, as shown in Figure 2(a). This is followed by deposition of low stress polysilicon which is patterned with photoresist (Figure 2(b)) and etched to define the microstructure (Figure 2(c)). A wet etch in hydrofluoric acid removes the sacrificial PSG layer, and releases the resulting polysilicon structure (Figure 2(d)).

2.2. Suspended MEMS

Suspended MEMS are a class of microstructures that are attached to the silicon substrate via compliant flexures or rigid anchors. As a counter-example, rotary micromotors [17] are not considered suspended MEMS. The maturity of suspended MEMS is exemplified by the recent success of commercial microaccelerometers for automotive airbag deployment [18][19] and digital mirror displays for high-fidelity video projection [20]. The availability of accumulated design expertise,

integrated MEMS/electronics fabrication capabilities, and electromechanical CAD modeling tools has made the suspended-MEMS technology a suitable candidate for initial development of design methodologies for MEMS.

The prototypical example of a suspended-MEMS component is the folded-beam flexure microresonator shown in Figure 1. This specific topology was first described and analyzed by Tang [21]. It is used in resonator oscillators, in filters, and as a mechanical characterization test structure to measure Young's modulus of thin films. The central shuttle mass is suspended by two folded-beam flexures to form a mechanical mass-spring-damper system. The structural elements in this process are formed using a homogeneous, conducting, polysilicon film. The movable microstructure is fixed to the substrate at only two anchor points, which also act as electrical vias. Wet etching of the sacrificial oxide under the structure results in the spacer gap.

The electrostatic actuators used to drive the resonator in the x-direction are called 'comb drives,' and are made from a set of interdigitated comb fingers. The generated electrostatic force, due to the application of a voltage across the comb fingers, does not depend upon the displacement of the resonator (to first order). The folded-flexure suspension is designed to be compliant in the x-direction of motion and to be stiff in all other in-plane directions (*e.g.*, y and θ) to keep the comb fingers aligned.

The simplified schematic view of the resonator, shown in Figure 3, represents the device as an interconnected set of mixed-domain lumped-parameter elements: the shuttle mass, two folded-flexure springs, and two comb-finger actuators which are displayed as time-varying capacitors. Each of these elements serves both an electrical and mechanical role. A voltage source that drives one actuator is also included in the schematic. The mechanical anchor points, designated by notation similar to electrical ground, affect functional parameters such as the system modal frequencies.

2.3. Current Design Methodology

The suspended-MEMS design process involves electrical, mechanical and electromechanical energy domains, and can get exceedingly complex. One such complex system is an microaccelerometer, which can be built from a mass-spring-damper system similar to the microresonator. A natural hierarchy exists in such a system. The microaccelerometer is decomposable into transduction and electronic components. The transduction component includes mechanical transduction of acceleration into inertial force, via the accelerometer's mass, then to displacement via the spring compliance, followed by electromechanical transduction using a variable capacitor to obtain an electrical signal. The electronic component is needed for subsequent signal conditioning and for feedback control to ensure that the transducer is stabilized. Optimal design will involve simulation at various levels: system-level using a signal-flow model of the transduction and feedback components to ensure loop stability, component-level simulation using a Kirchhoffian lumped-parameter model of the transduction component to understand distortion and noise, and, device-level simulation using a meshed solid-model of the mechanical spring sub-component to understand the effect of process overetch on sensor performance. Therefore, MEMS design truly involves the range from system design, in which the application domain constrains the designer, to device design, in which the manufacturing technology constrains the designer.

Most MEMS design currently takes place at the device level. MEMS engineers begin the process of designing a new component with a rough sketch and very basic equations to ensure feasibility. This stage usually leads directly to a physical layout, due to the tight integration of form and function in the mechanical domain. This physical layout, the microfabrication process flow, and the materials properties of the materials used in the microfabrication process determine the actual performance of the final design. The designer currently has two choices for pre-fabrication design verification: numerical simulation (*e.g.,* finite-element analysis), and behavioral simulation.

6

Numerical simulation involves self-consistent mechanical finite-element analysis coupled with electrostatic boundary-element analysis. Tools that cater to the MEMS community are available from several companies [22][23][24]. The modeling of the design (solid model and meshing) for numerical simulation, and the subsequent interpretation of simulation results requires domain expertise and quickly becomes tedious. Furthermore, these simulation strategies can only verify mechanical or electromechanical operation, and do not allow the complete simulation of the microelectromechanical component with its attendant electronics. Therefore, numerical simulation is primarily seen as critically important for MEMS modeling and verification, analogous to the role that technology CAD plays in electronic device and interconnect modeling.

The device designer who understands the microelectromechanical design and technology issues needs to capture and encapsulate the detailed device behavior into a representation that the system engineer can understand [25][26]. The system engineer is an expert on the final system application (for example, the accelerometer system). Approaches to encapsulating device behavior into a behavioral representation suitable for system-level simulation have been proposed [27]. Behavioral simulation can then be accomplished using many different commercial tools, such as SPICE [28] and MATLAB [29]. The encapsulation of device behavior into a "black-box" model is limited to fixed geometry, hence the system engineer is unable to evaluate all the trade-offs affecting the system-level performance.

The above methodology captures system design details in a bottom-up fashion. Fixed, and geometric parametrized component libraries to support this methodology have been constructed [30][31], to enable design reuse. Behavioral models for fixed components in the component library have been developed, allowing the system designer to choose between alternate components, depending on system trade-offs. However, since the number of MEMS design specifications tends to be quite large (on the order of tens of specifications compared to a couple for a digital

component or leaf-cell), no fixed component library can ever capture the complete range of specifications of interest to the system-level designer. Parameterized layout-based libraries have been developed to address this issue, but as of yet, they do not have associated parametrized models, thus their use is still limited to device designers intimately familiar with suspended-MEMS technology.

No rapid design process is available today for systems incorporating MEMS. Although device verification via numerical simulation is now standard, few (complete system) design verification iterations are usually attempted during prototype design, resulting in fabrication replacing simulation in the iterative design loop. This is very expensive, since fabricated prototypes often do not meet performance specifications and, sometimes, are not even functional. These problems inhibit the use of MEMS for low-cost, low-volume application specific sensors, integrated on the same chip with electronic information processing and communication capabilities.

3. MEMS Abstractions

To enable the design of systems monolithically integrating MEMS and electronics, this paper proposes a *hierarchical top-down* design methodology [32][33][34][35] based on existing digital and analog design methodologies. Other researchers have proposed similar methodologies [36][37][38][39]. A successful design methodology must recognize the levels of abstraction possible in the design process. The resulting design partitioning allows the application-knowledgeable system designer, the MEMS component engineer and the technology-conscious process/device engineer to collaborate in designing the final product. In particular, hierarchical abstractions enable the system designer to focus on the application given the component constraints and a simple parametric model of the technology.

In the digital VLSI domain, system designers use high-level behavioral representations to describe their design, and to reason about the design's functionality. This is then mapped into a structural representation, where critical issues regarding the design's performance can be solved. Technology mapping into a logic-level representation further clarifies the details of the design, and physical design renders the design into the mask information required for its manufacture. The analog VLSI domain is not quite as clean. Behavioral (or signal flow) representations can be developed to understand the impact of issues like noise and non-linearity. Although manual technology mapping into the circuit (*i.e.*, Kirchhoffian) domain is currently required to actually complete the design, there are several emerging approaches to meeting the performance goals given a circuit topology (*i.e.*, structural representation of function) [40]. Due to the coupling of physical layout issues into the device performance, careful manual layout is still required, although again, there are emerging approaches that automate the care a layout technician gives to the circuit [41].

The MEMS domain is considered by many to be more difficult than the analog domain. At least the analog circuit designer has the advantage of lumped-element MOS models for use in Kirchhoffian simulation. The MEMS designer on the other hand has a long history of relying on distributed finite and boundary element models. However, due to the underlying IC fabrication techniques, most MEMS structures may be abstracted to a higher level. As in circuit design, a schematic representation of MEMS provides a critical link between layout and behavioral simulation that enables high-level design automation. The schematic representation involves lumped-parameter models of elements commonly found in suspended MEMS. For example, the folded-flexure resonator in Figure 4(a) is considered a *component* in an oscillator. In Figure 4(b), the resonator is partitioned into *functional elements:* a shuttle mass, two symmetrical folded-flexure springs and two comb drives. These functional elements are composed of reusable *atomic elements* such as the anchor, plate, beam and electrostatic gap shown in Figure 4(c). All existing sus-

9

pended-MEMS designs can be partitioned into similar atomic elements. Conversely, new components higher up in the hierarchy can be formed from the lower-level elements, and these in turn can be used in even higher-level components and systems. Tools for mixed-domain circuit simulation, synthesis and extraction to support this hierarchy will now be discussed.

4. Mixed-Domain Circuit Simulation

The ability to perform hierarchical multi-domain circuit simulation of electronics with MEMS empowers component-level and system-level designers to explore the trade-offs affecting performance. Our approach to mixed-domain circuit simulation uses a simple set of microelectromechanical elements, which can be hierarchically interconnected to create more complicated components and systems [42][43][44]. Values of all electrical, mechanical, and electromechanical variables under the designer's control are visible and can be changed in the mixed-domain schematic.

Pister at U. C. Berkeley [45][46] is developing a similar hierarchical representation and researchers at Bosch, GmbH are applying a similar methodology, although optimized for the design of their gyroscope [47][48]. MEMS design representations with varying degrees of abstraction for hierarchical construction of suspended MEMS are available in several CAD frameworks [39][49][50][51].

The lowest level in MEMS circuit hierarchy comprises a handful of atomic elements such as anchors, beams, plates and electrostatic gaps. Element schematic symbols are icons that mimic the layout view, and have the appropriate port view for mechanical and electrical connections to other elements. The atomic elements include physical behavioral models for support of mixed-domain circuit simulation. The elements integrate form and function as part of their mechanical nature, therefore, physical placement parameters must be included in the underlying models. For exam-

ple, physical placement of beams and plates affect the resonant modes of microstructural components.

Currently, behavioral models of the atomic elements are implemented in analog-HDL with displacements and forces acting in the *x-y* plane of the wafer [52][53]. An example of a beam element connected to an anchor (*i.e.*, a cantilever) is depicted in Figure 5. In-plane translational displacement (*x, y*) and rotational displacement (θ) are defined as across variables. Forces (F_x, F_y) and bending moment (M_θ) acting on the element are defined as through variables. This treatment of mechanical variables is similar to treating voltages (*V*) as across variables and currents (*I*) as through variables in an electrical circuit. The force balance equation, which states that the sum of all forces acting on a body is zero, is enforced by the mechanical equivalent of Kirchhoff's current law. That is, the sum of all "branch forces" incident at a node is equal to zero. The beam model specifies the constitutive relation for the force *vs.* displacement, based on well-known elastic theory [54]. In the mixed-domain schematic in Figure 5(b), a force is applied at the end of the beam in the *y*-direction, resulting in a translational and rotational displacement.

To increase the speed of simulation, reduced-order macromodels of selected higher-level components may be developed. An one-dimensional version of the comb-drive model is shown in Figure 6. The comb drive is both a capacitive sensor and an electrostatic actuator. The air-gap capacitance across the interdigitated comb fingers is modeled as a displacement-dependent capacitor, C. A first-order model, based on parallel-plate capacitance and valid when the fingers overlap, is

$$C = \frac{2N\varepsilon_o h}{g}(x_o - x) \tag{1}$$

where ε_o is permittivity of air, *h* is the comb-drive thickness, *g* is the gap between fingers, *N* is the number of rotor fingers, and x_o is the finger overlap at rest. The capacitance decreases linearly

11

with the displacement, x. If a voltage is applied across the comb drive, a motion of the fingers will generate electrical displacement current arising from the change in charge ($q = C V$) with time. The application of a voltage will also generate an electrostatic force in the x-direction as defined by the dependent through-variable source, F. The force is a non-linear function of voltage, given to first-order by

$$F = \frac{1}{2}\frac{\partial C}{\partial x}V^2 = -\frac{N\varepsilon_o h}{g}V^2 \tag{2}$$

where V is the applied voltage across the comb drive. The force source attracts the rotor set of movable fingers to the stator set of anchored fingers.

A mixed-domain schematic of a folded-flexure microresonator is shown in Figure 7. In this topology, the resonator component is represented as a connected set of 14 beams, five plates, six anchors and two comb-drive elements. The two key features of the representation are the one-to-one correspondence of physical layout to the low-level elements, and the easy integration into existing IC schematic capture tools.

The microresonator was simulated in Saber^{TM}[55] using two-dimensional models [44]. Transient and a.c. simulation results are shown in Figure 8. From the ac sweep simulation, the mechanical resonant frequency is 30 kHz. Since the resonant frequency is determined solely by the elastic properties of the resonator, a numerical finite element analysis of a solid model of the resonator was performed to verify the circuit simulation accuracy. The results agree to within 1%, with the circuit simulation taking several seconds compared to a few minutes for the finite element analysis. More importantly, input preparation (layout to solid model generation and meshing) took almost an afternoon for the finite element analysis, whereas the layout-based schematic was constructed from the atomic and functional elements in about ten minutes.

The mixed-domain circuit simulation is able to generate transient simulation results of integrated MEMS with electronics, which is not possible in the finite element analysis. The transient simulation indicates that the steady-state drive amplitude is 2.5 μm with a start-up settling time of 3 ms.

The microresonator example is prototypical of suspended-MEMS applications such as resonator oscillators, micromechanical RF filters, capacitive accelerometers and capacitive vibratory-rate gyroscopes. These systems share common traits of suspended mass, electrostatic actuation, capacitive motion detection, and conditioning and control electronics. Transient, d.c. and a.c. simulation capability for these mixed-domain systems is crucial for evaluating their performance. Since the mixed-domain circuit representation fits into existing simulation environments, the designer can take advantage of Monte-Carlo and worst-case analysis capabilities built into the tools.

5. Layout Synthesis of MEMS Components

MEMS components tend to have a large number of design specifications coupled with large ranges for each specification. For example, the acceleration specification for microaccelerometer applications ranges from 1 G for inertial sensors to greater than 100,000 G for munitions fuzing. Additional specifications, including bandwidth, resolution, sensitivity, linearity, and cross-axis rejection, must be simultaneously satisfied for a specific application. This limits the usefulness of fixed-cell libraries in MEMS design.

Although parametrized component libraries have been developed (*e.g.*, CaMEL from MCNC [31]), the component generators are purely geometric, therefore the designer must manually evaluate numerous iterations to generate a design which satisfies performance requirements. An alternate approach to generating such a design is to use design optimization to invert the design analysis equations, given a list of desired performances. Design optimization tools have been

13

developed for important classes of MEMS components such as compliant mechanisms (flexible structures that generate a wide variety of mechanical motions through elastic deformations) [56][57], spring/active area trade-offs [58], comb-drives [59], and bulk micromachined structures [60]. Our approach [61][62] combines geometric parametrized cell-library generation with design optimization to translate the user-specified device specifications (*e.g.*, resonator frequency) directly into geometrical layout parameters. Synthesis modules for commonly used suspended-MEMS components, such as resonators [63], accelerometers [64], gyroscopes and positioners are being developed. Instead of redesigning these components each time a new system is proposed, engineers benefit from synthesizers which tackle the routine design of frequently-used components. From the system designer's point of view, such synthesizers take care of all the technology and device issues, and allow the designer to focus on the component performance, and its impact on system performance.

The development of a synthesis module involves determining the design variables, the numerical design constraints, and the quantitative design objective. As a starting point, a synthesis tool for the surface-micromachined resonator topology of Figure 1 has been developed and tested. The lowest nine lateral translational and rotational modes (both in-plane and out-of-plane) of the mass-spring-damper system are modeled by second-order equations of motion. In this initial work, analytical equations are used instead of the mixed-domain circuit simulation methodology detailed in Section 4 because of the prohibitively long time required by the iterative nature of optimization-based synthesis. In essence, these equations model the behavior of the functional elements (*e.g.*, folded-flexure spring, comb drive), rather than the atomic elements (*e.g.*, beams and gaps). This higher level modeling results in the elimination of internal nodes from the mixed-domain circuit simulation, and a faster performance evaluation module for the iterative synthesis methodology.

In the *x*-direction, the second-order lumped-parameter mass-spring-damper system is:

$$F_{e,x} = m_x \ddot{x} + B_x \dot{x} + k_x x \tag{3}$$

where $F_{e,x}$ is the lateral component of the external electrostatic force generated by the comb drives. The effective mass (m_x), damping coefficient (B_x), and spring constants (k_x) for these modes are calculated from the geometry and material parameters of the lumped elements. Similar equations are derived for the other lateral translational and rotational modes. The coefficients in (3) can be expanded to:

$$m_x = m_s + \frac{1}{4}m_t + \frac{12}{35}m_b \tag{4}$$

where m_s is the shuttle mass, m_t is the total mass of all truss sections, and m_b is the total mass of all long beams. For operation at atmospheric pressure, damping is dominated by viscous air forces generated by the moving shuttle. Viscous air damping is proportional to velocity with a damping factor given by [65]:

$$B_x = \mu \left[(A_s + 0.5A_t + 0.5A_b)\left(\frac{1}{d} + \frac{1}{\delta}\right) + \frac{A_c}{g} \right] \tag{5}$$

where μ is the viscosity of air, d is the spacer gap, δ is the penetration depth of airflow above the structure, A_c is the gap between comb fingers, and A_s, A_t, A_b, and A_c are bloated layout areas for the shuttle, truss beams, flexure beams, and comb-finger sidewalls, respectively. Linear equations for the folded-flexure spring constants in the x-direction is given by [66]:

$$k_x = \frac{2Etw_b^3}{L_b^3} \frac{L_t^2 + 14\alpha L_t L_b + 36\alpha^2 L_b^2}{4L_t^2 + 41\alpha L_t L_b + 36\alpha^2 L_b^2} \tag{6}$$

where E is the Young's modulus of polysilicon, t is the polysilicon thickness and α is the cube of ratio of the beam to truss width.

All of the design variables are structural parameters of the folded-flexure and comb-drive elements, with the exception of the comb-drive voltage. Technology-driven design rules constrain the

minimum geometries, such as beam widths and minimum spaces between structures. Maximum values of structural parameters are primarily constrained by manufacturing constraints such as sticking of the structural film to the substrate during sacrificial oxide etching. The functional constraints include resonant frequency, stroke, quality factor, and electromechanical stability.

The complete design problem (described in detail in [67]) is represented as a constrained nonlinear optimization problem, and solved by an off-the-shelf solver [68]. A gridded-multistart approach is used to overcome local minima, and a branch-and-bound approach is used for handling the integer variables (*e.g.*, number of comb fingers). Various design objectives such as minimization of area, drive voltage, combination of area and voltage, and maximization of displacement have been used to explore the resonator design space. Various engineering specifications such as resonator frequency were used to understand the constraint space for each microresonator objective. Results for low-frequency (10 kHz) and high-frequency (300 kHz) resonators are shown in Figure 9. As expected, the high frequency devices are much smaller than their low frequency counterparts. Smaller devices have less mass, and smaller flexures are stiffer. Both effects increase the resonant frequency.

Synthesized resonators were experimentally fabricated to verify their actual resonant frequencies and quality factors and compared to the analytical model. The fabricated resonators were affected by beam overetching, resulting in a trapezoidal cross-section with beam widths being smaller than the designed values. Using measured results for the trapezoidal cross-section geometry and material properties, the analytically predicted values of resonant frequency and quality factor are compared to the corresponding experimental results in Figure 10. The analytical models are quite accurate with the measured resonant frequency matching to within 4% of the model. This implies that the synthesis tool is able to synthesize resonators with intended resonant frequencies, if a process that has a well-characterized overetch is used.

16

The quality factor is accurate to about 20% at high frequencies (at 20 kHz, the model is accurate to within 5%). At higher frequencies, when the dimensions are small, the edge and finite-size damping effects become more significant. Hence, more error in the quality factor model is seen at higher frequencies. Higher accuracy requires research on more accurate MEMS damping models.

6. MEMS Layout Extraction

Layout correctness can only be accomplished by extracting the layout into a schematic netlist and simulating for functional correctness, or by comparing the layout to a golden design netlist to ensure geometric connectivity [69]. The VLSI design methodology also uses extraction for layout verification. Unlike VLSI, the features (shape, size and position) of each layout rectangle is of utmost importance and plays a crucial role in recognizing the constitutive MEMS elements.

The objective of the extraction tool is to recognize the layout elements based on their geometric features, enabling subsequent rapid simulation-based verification. To achieve this, the lowest-level atomic elements are first detected followed by recognition of commonly used functional elements such as comb drives. Since the parameterized models for these elements were already derived for mixed-domain circuit simulation, the layout extraction only needs to determine the geometrical parameters of the identified elements.

The extraction process is demonstrated using the folded-flexure resonator layout shown in Figure 11(a). The input layout is converted into a canonical representation, shown in Figure 11(b), which allows the development of algorithms that are independent of the CAD software used to generate the input layout. The canonical representation significantly increases the number of rectangles needed to represent the design, primarily because of the presence of fingers in the resonator layout. Suspended MEMS tend to use a significant number of fingers to improve electromechanical transduction. Identification and elimination of the fingers results in an alternative canonical

17

representation that is greatly simplified (Figure 11(c)). Feature-based recognition then detects the various atomic elements (beams, plates, gaps and anchors) as shown in Figure 11(d). Technology-specific information from other layers, like location of anchor cuts, is used to help in this phase. In Figure 11(e), each of the remaining rectangles in the canonical representation are classified using properties of the elements (*e.g.*, a beam is a rectangle with two ports located on its two short sides) and using the interconnectivity between the elements. The next step is to reduce the number of rectangles needed to represent the mass and anchor area. Figure 11(f) shows a minimal representation where the rectangles have been first merged horizontally and then merged vertically. This merging reduces the total number of ports in the generated netlist, and hence decreases the simulation time for the extracted netlist. The minimized set of classified rectangles is then converted into a netlist. The geometric size of each of the classified rectangles is extracted into the element parameters in this netlist. The primary objective of having a check on the designed layout is achieved by comparing the extracted netlist with the original design netlist. Behavior may also be verified by running a mixed-domain circuit simulation on the extracted netlist.

The present implementation is limited to Manhattan-style (rectilinear) designs. Therefore, the extracted parameters for each rectangle are simply its center position, length and width. Furthermore, the rectangle identification routine is technology specific, and the present implementation is limited to the MUMPS polysilicon MEMS process. Extensions to other polysilicon MEMS processes is trivial.

7. Discussion

The mixed-domain circuit simulation, synthesis and extraction tools form the core of a top-down integrated electronics/MEMS design methodology. In this hierarchical design methodology, the system-level engineer begins by creating a system architecture that implements the desired

system concept, as shown in Figure 12. A general mixed-domain architecture will include digital electronics for computation, analog electronics for signal conditioning and control, RF electronics for communication, and MEMS for sensing, control, and actuation. A traditional digital design approach can be followed for the digital portion of the design. Emerging analog design methodologies [70] and RF design tools can be applied for the analog and RF portion of the design problem, with the MEMS designed via an electronics-compatible MEMS design flow.

At the topmost level, the MEMS system needs to be manually decomposed into components that when combined achieve the functionality of the system, just like in the analog domain (unlike the digital arena, where behavioral synthesis of desired function is possible). For the resonator oscillator example, the components include the transducer and capacitive-sense electronics. Past achievable component performances together with design creativity at the system-level guides the final architecture choices. Behavioral models of the components in analog HDL such as VHDL-AMS [71] can be simulated to determine the component specifications needed to meet the target system goals. These models are behavioral (*i.e.*, a second-order transfer function) and not structural (*i.e.*, the mass-spring-damper topology is unspecified), and therefore are easily created manually.

The MEMS components in the system architecture need to be refined into a structural representation. Structural representation of digital blocks can occur at several levels (RTL, logic, gate, switch, circuit). The layout-based schematic of Section 4 provides the structural representation for the MEMS components (*e.g.*, the resonator), and can be integrated with electronics to represent the entire system (*e.g.*, an oscillator). A mixed-domain circuit simulation can be used to explore alternate connections of mechanical, electromechanical and electronic elements to determine the component topology. Once a MEMS component topology is chosen, the sizes of each atomic element need to be determined. The component-synthesis tool of Section 5 translates the compo-

19

nent's performance specifications into layout, enabling a system-designer to design the optimum MEMS components needed for the system. Alternately, this sizing task can be performed by iterating on the mixed-domain circuit simulation (which can be easily translated into the actual layout since the schematic is layout-based).

The next step is the verification of the component layout, which is accomplished via the layout extraction tool of Section 6. Extraction leads to a simulation netlist, that is verified for functionality via mixed-domain circuit simulation. Finally, the component layouts can be integrated into a system layout (using a traditional electronics floorplanner and chip-level router for now, until the demands that integrated electronics/MEMS systems are better understood). System-level extraction and simulation for the integrated electronics/MEMS is needed to verify functional correctness, and may result in design iterations prior to fabrication. Again, traditional hierarchical electronics extraction tools will suffice for now (until a more complete understanding of coupling and parasitics between MEMS blocks within an integrated microsystem is achieved). As hierarchical electronic extraction tools are unable to identify the MEMS elements, the first step in system-level extraction involves a MEMS extraction, in which the atomic elements, functional elements and MEMS components are identified, and appropriately annotated into the layout for subsequent extraction via traditional electronics extraction tools.

One crucial issue is the back-annotation of technological information from the component-level to the system-level. The initial architecture exploration and component specifications are developed using simplistic behavioral models. These models have to be elaborated with response surface models that capture the actual component performances for system-level verification. Several alternatives for this back-annotation are currently being explored, and no conclusive results are available at this stage.

8. Conclusions

 The mixed-domain systems-on-a-chip design methodology for suspended MEMS promises to shorten the development cycle to days, and enable design of more complex systems comprised of hundreds to thousands of micromechanical elements. Identification of reusable hierarchical representations of MEMS components is a critical first step in advancing toward a hierarchical design methodology and in leveraging existing CAD tools.

A mixed-domain schematic representation and circuit simulation technique enables rapid exploration and analysis of the design space for MEMS components. The identification and modeling of the fundamental MEMS elements, and the ability to interconnect these elements for new device designs is critical for the shortening the MEMS design cycle.

MEMS component synthesis is a powerful tool for building common components that can then be used in larger systems. The identification and modeling of component-level lumped-parameter models that adequately link device behavior with physical design variables, and the integration of these models with optimization leads to automatic custom design capability, as well as design-space exploration capability crucial for the system-level architecture decisions.

MEMS extraction is essential for layout verification of synthesized or manual layouts. The use of a common set of fundamental elements between the extraction and simulation methodologies enables the use of extraction output for behavioral verification, as well as for netlist comparison to ensure correct connectivity of the components.

Finally, we envision a MEMS design environment in which the expert MEMS designer can rapidly iterate on ideas for MEMS designs, in the same integrated environment where a system-level designer can use synthesized and custom-made MEMS components to develop monolithic mixed-technology chips for low-cost, low-volume applications. Such an environment is essential for

designs in which several unique MEMS sensors need to be integrated on the same chip with electronic information processing capability.

9. Acknowledgment

10. References

[1] R. T. Howe, R. S. Muller, K. J. Gabriel, W. S. N. Trimmer, "Silicon micromechanics: sensors and actuators on a chip," *IEEE Spectrum*, vol.27, no.7, p. 29-31, 34-35.
[2] J. Bryzek, K. Petersen, and W. McCulley, "Micromachines on the March," *IEEE Spectrum*, May 1994, pp. 20-31.
[3] S. T. Picraux and P. J. McWhorter, "The broad sweep of Integrated Microsystems," *IEEE Spectrum*, December 1998, pp. 24-33.
[4] N. Yazdi, F. Ayazi, and K. Najafi, "Micromachined Inertial Sensors," *IEEE Proceedings*, pp. 1640-1659, Aug, 1998.
[5] P. F. Van Kessel, L. J. Hornbeck, R. E. Meier, and M. R. Douglass, "A MEMS-based Projection Display," *IEEE Proceedings*, pp 1687-1704, Aug, 1998.
[6] T. D. Boone, H. H. Hooper, D. S. Soane, "Integrated Chemical Analysis on Plastic Microfluidic Devices," in *Proc. of Solid State Sensors and Actuators Workshop*, Hilton Head, SC, June 8-11, 1998, pp. 87-92.
[7] G. Asada, M. Dong, T.S. Lin, F. Newberg, G. Pottie, W.J. Kaiser, and H.O. Marcy. "Wireless Integrated Network Sensors: Low Power Systems on a Chip," in *Proc. of the 1998 European Solid State Circuits Conference*.
[8] M. Despont, J. Brugger, U. Drechsler, U. Durig, W. Haberle, M. Lutwyche, H. Rothuizen, R. Stutz, R. Widmer, H. Rohrer, G. Binnig, and P. Vettiger, "VLSI-NEMS Chip for AFM Data Storage," in *Proc. of 1999 IEEE Microelectromechanical Systems Conference*, Orlando, FL, Jan 17-21, 1999, pp. 564-569.

[9] W.C. Tang, "Overview of Microelectromechanical Systems and Design Processes," in *Proc. of 34th Design Automation Conference,* Anaheim, CA, June 9-13, 1997, pp. 670-3.

[10] D.A. Koester, R. Mahadevan, K.W. Markus, *Multi-User MEMS Processes (MUMPs) Introduction and Design Rules,* available from MCNC MEMS Technology Applications Center, 3021 Cornwallis Road, Research Triangle Park, NC 27709, rev. 3, Oct. 1994, 39 pages.

[11] Intelligent Micro Machine Initiative, Sandia National Laboratories, http://www.mdl.sandia.gov/micromachine/.

[12] J. H. Smith, S. Montague, J. J. Sniegowski, J. R. Murray, and P. J. McWhorter, "Embedded micromechanical devices for the monolithic integration of MEMS with CMOS," in *Proc. IEDM,* 1995, pp. 609-612.

[13] *Introduction to iMEMS^{TM}*, Analog Devices, Inc., (http://imems.mcnc.org/imems/imems.html

[14] H. Baltes, O. Paul, O. Brand, "Micromachined Thermally Based CMOS Microsensors," *Proceedings of the IEEE*, vol. 86, no. 8, pp. 1660-78.

[15] G. K. Fedder, S. Santhanam, M. Reed, S. Eagle, M. Lu, R. Carley, "Laminated High-Aspect-Ratio Microstructures in a Conventional CMOS Process," *Sensors and Actuators* A, 57 pp 103-110 (1996).

[16] J. M. Bustillo, R. T. Howe and R. S. Muller, "Surface Micromachining for Microelectromechanical Systems," *Proceedings of the IEEE*, vol. 86, no. 8, pp. 1552-74.

[17] M. Mehregany, S. D. Senturia, J. H. Lang and P. Nagarkar, "Micromotor Fabrication," *IEEE Transactions on Electron Devices*, vol. 39, no. 9, pp. 2060-9

[18] *ADXL250 Accelerometer Data Sheet,* Analog Devices, Inc., One Technology Way, P.O.Box 9106, Norwood, MA 02062-9106, 1998 (http://www.analog.com).

[19] *PMMA2001D Accelerometer Data Sheet,* Motorola Sensor Products, 1998 (http://design-net.com/senseon).

[20] *DLP Data Sheets*, Texas Instruments DLP Division, 1998 (http://www.ti.com/dlp/)

[21] W. C. Tang, T.-C. H. Nguyen, M. W. Judy, and R. T. Howe, "Electrostatic comb drive of lateral polysilicon resonators," *Sensors and Actuators A*, vol.21, no.1-3, pp. 328-31, Feb. 1990.

[22] *MEMCAD Web Page,* http://www.memcad.com, Microcosm Technologies, Inc., 201 Willesden Dr., Cary, NC 27513.

[23] *Intellisense Web Page,* http://www.intellis.com, IntelliSense Corporation, 16 Upton Dr., Wilmington, MA 01887.

[24] J. M. Funk, J. G. Korvink, J. Bühler, M. Båchtold, and H. Baltes, "SOLIDIS: A Tool for Microactuator Simulation in 3-D," *J. of Microelectromech. Sys.*, v. 6, no. 1, pp. 70-82, March 1997. (*SOLIDIS Web Page,* http://www.ise.ch/solidis)

[25] S. D. Senturia, "CAD Challenges for Microsensors, Microactuators and Microsystems," *Proceedings of the IEEE*, vol. 86, no. 8, pp. 1611-1626, Aug. 1998.

[26] S. D. Senturia, "Simulation and design of microsystems: a 10-year perspective," *Sensors and Actuators A*, 70 (1998), pp. 1-7.

[27] L. D. Gabbay and S. D. Senturia, "Automatic Generation of Dynamic Macro-Models?," in *Proc. 1998 Solid State Sensors and Actuators Workshop*, Hilton Head, GA, June 7-11, 1998.

[28] G. K. Fedder and R. T. Howe, "Multimode Digital Control of a Suspended Polysilicon Microstructure," *J. of Microelectromechanical Systems*, pp 283-297, Vol 5., No. 4, December 1996.

[29] G. K. Fedder, *Simulation of Microelectromechanical Systems*, Ph.D. Thesis, Dept. of Electrical Engineering and Computer Science, U. C. Berkeley, Sept. 1994.

[30] *Micromachines Program*, available from Multi-Project Circuits (CMP) Service, 46, avenue Felix Viallet, 38031 Grenoble Cedex, Oct. 1994, 29 pages.

[31] *CaMEL Web Page*, http://www.mcnc.org/camel.org, MCNC MEMS Technology Applications Center, 3021 Cornwallis Road, Research Triangle Park, NC 27709.

[32] T. Mukherjee and G. K. Fedder, "Structured Design of Microelectromechanical Systems," in *Proc. of 34th Design Automation Conference*, Anaheim, CA, June 9-13, 1997, pp. 680-685.

[33] R. D. Blanton, G. K. Fedder and T. Mukherjee, "Hierarchical Design and Test of MEMS," *MST News*, vol. 1, 1998.

[34] T. Mukherjee and G.K. Fedder, "Design Methodology for Mixed Domain Systems on a chip," in *Proc. IEEE Computer Society Workshop on VLSI 98*, Orlando FL, April 1998, pp. 96-101.

[35] G. K. Fedder, "Structured Design of Microelectromechanical Systems," in *Proc. IEEE Int. Conf. on Microelectromechanical Systems*, Orlando, FL, Jan. 18-21, 1999, pp. 1-8.

[36] E.K. Antonsson, "Structured Design Methods for MEMS," *NSF Sponsored Workshop on Structured Design Methods for MEMS*, November 12-15, 1995.

[37] E. C. Berg, N. R. Lo, J. N. Simon, H. J. Lee, K. S. J. Pister, "Synthesis and Simulation for MEMS Design", *ACM SIGDA Physical Design Workshop, Reston VA, April 1996*, pp. 66-70.

[38] N. R. L. Lo, E. C. Berg, S. R. Quakkelaar, J. N. Simon, M. Tachiki, H.-J. Lee, and K. S. J. Pister, "Parametrized Layout Synthesis, Extraction, and SPICE Simulation for MEMS," in *Proc. 1996 IEEE International Symposium on Circuits and Systems*, pp 481-484, Atlanta, GA, May 12-15, 1996.

[39] J. M. Karam, B. Courtois, H. Boutamine, P. Drake, A. Poppe, V. Szekely, M. Rencz, K. Hoffman, M. Glesner, "CAD and Foundries for Microsystems," in *Proc. of 34th Design Automation Conference*, Anaheim, CA, June 9-13, 1997, pp. 674-679.

[40] E. S. Ochotta, T. Mukherjee, R. A. Rutenbar, and L. R. Carley, *Practical Synthesis of High-Performance Analog Circuits*, Kluwer Academic Publishers, 1997.

[41] J. M. Cohn, D. J. Garrod, R. A. Rutenbar and L. R. Carley, *Analog Device-Level Layout Automation*, Kluwer Academic Publishers, 1992.

[42] J. E. Vandemeer, M. S. Kranz, and G. K. Fedder, "Nodal Simulation of Suspended MEMS with Multiple Degrees of Freedom," in *Proc. of the 1997 International Mechanical Engineering Congress and Exposition: The Winter Annual Meeting of ASME in the 8th Symposium on Microelectromechanical Systems*, Dallas, TX, Nov. 16-21, 1997.

[43] J. E. Vandemeer, M. S. Kranz, and G. K. Fedder, "Hierarchical Simulation of Surface-Micromachined Inertial Sensors," in *Proc. 1998 Int. Conf. on Modeling and Simulation of Microsystems, Semiconductors, Sensors and Actuators (MSM '98)*, Santa Clara, CA, April 6-8, 1998, pp. 540-5.

[44] G. K Fedder and Q. Jing, "NODAS 1.3 - Nodal Design Of Actuators And Sensors," in *Proc. IEEE/VIUF Int. Workshop on Behavioral Modeling and Simulation*, Orlando, FL, October 27-28, 1998.

[45] J. Clark, N. Zhou, S. Brown and K.S.J. Pister, "Nodal Analysis for MEMS Design Using SUGAR v0.5," in *Proc. 1998 International Conference on Modeling and Simulation of Microsystems, Semiconductors, Sensors and Actuators (MSM 98)*, Santa Clara, CA, April 6-8, 1998, pp. 308-13.

[46] J. Clark, N. Zhou, and K.S.J. Pister, "Fast, Accurate MEMS Simulation with SUGAR 0.4," in *Proc. 1998 Solid State Sensors and Actuators Workshop*, Hilton Head, GA, June 7-11, 1998.

[47] G. Lorenz and R. Neul, "Network Modeling of Micromachined Sensor Systems," in *Proc. 1998 International Conference on Modeling and Simulation of Microsystems, Semiconductors, Sensors and Actuators (MSM 98)*, Santa Clara, CA, April 6-8, 1998, pp. 233-8.

[48] D. Teegarden, G. Lorenz and R. Neul, "How to model and simulate microgyroscope systems," *IEEE Spectrum*, Vol 35, No. 7, pp. 66, 1998.

[49] M. A. Maher and H. J. Lee, "MEMS Systems Design and Verification Tools," in *Proc. of the SPIE Smart Structures and Materials Conference*, San Diego, CA, March 1998, pp. 40-48.

[50] N. Swart, S. F. Bart, M. H. Zaman, M. Mariappan, J. R. Gilbert, and D. Murphy, "Auto-MM: Automatic Generation of Dynamic Macromodels for MEMS Devices," in *Proc. of the IEEE Micro Electro Mechanical Systems Workshop*, Heidelberg, Germany, pp.178-183, Jan. 1998.

[51] J. Scholliers, T. Yli-Pietila, "Simulation of Mechatronic Systems Using Analog Circuit Simulation Tools", in *Proc. IEEE Intl. Conference on Robotics and Automation*, Nagoya, Japan, 21-27May 1995, vol. 3, pp. 2847-52.

[52] I. Getreu, "Behavioral Modeling of Analog Blocks using the SABER Simulator," in *Proc. Microwave Circuits and Systems*, pp 977-980, August 1989.

[53] Open Verilog International, "Verilog-A reference manual: Analog extensions to Verilog-HDL," http://www.ovi.org.

[54] S. P. Przemieniecki, *Theory of Matrix Structural Analysis,* McGraw-Hill, New York, New York, 1968.

[55] I. Getreu, "Behavioral Modelling of Analog Blocks using the SABER Simulator," in *Proc. Microwave Circuits and Systems*, pp. 977-980, August 1989.

[56] G.K. Ananthasuresh, S. Kota, and N. Kikuchi, "Strategies for Systematic Synthesis of Compliant MEMS," in *Proc. 1994 ASME Winter Annual Meeting*, *Dynamics Systems and Control,* Chicago, IL, DSC-Vol. 55-2, pp. 677-686.

[57] A. Saxena and G. K. Ananthasuresh, "An Optimality Criteria Approach for the Topology Synthesis of Compliant Mechanisms," in *Proc. 1998 ASME Design Engineering Technical Conferences (DETC '98) - 25th Biennial Mechanisms Conference*, paper DETC98/MECH-5937, Atlanta, Sept. 1998.

[58] D. Haronain, "Maximizing microelectromechanical sensor and actuator sensitivity by optimizing geometry", *Sensors and Actuators A*, 50(1995), pp. 223-236.

[59] W. Ye, S. Mukherjee, and N.C. MacDonald, "Optimal Shape Design of an Electrostatic Comb Drive in Microelectromechanical Systems", *J. Microelectromechanical Systems*, March 1998, vol. 7, pp. 16-26.

[60] H. Li and E. L. Antonsson, "Evolutionary Techniques in MEMS Synthesis," in *Proc. 1998 ASME Design Engineering Technical Conferences (DETC '98) - 25th Biennial Mechanisms Conference*, paper DETC98/MECH-5840, Atlanta, Sept. 1998.

[61] G. K. Fedder, S. Iyer, and T. Mukherjee, "Automated Optimal Synthesis of Microresonators," in *Technical Digest of the IEEE Int. Conf. on Solid-State Sensors and Actuators (Transducers '97)*, Chicago, IL, June 16-19, 1997, v. 2, pp. 1109-1112.

[62] S. Iyer, T. Mukherjee, and G. K. Fedder, "Multi-Mode Sensitive Layout Synthesis of Microresonators," in *Proc. 1998 Int. Conf. on Modeling and Simulation of Microsystems Semiconductors, Sensors and Actuators (MSM '98)*, Santa Clara, CA, April 6-8, 1998, pp. 392-7.

[63] T. Mukherjee, S. Iyer, and G. K. Fedder, "Optimization-based synthesis of microresonators," *Sensors and Actuators A*, 70 (1998), pp 118-127.

[64] T. Mukherjee, Y. Zhou, and G. K. Fedder, "Automated Optimal Synthesis of Microaccelerometers," in *Proc. IEEE Int. Conf. on Microelectromechanical Systems*, Orlando, FL, Jan. 18-21, 1999, pp. 326-31.

[65] X. Zhang and W. C. Tang, "Viscous Air Damping in Laterally Driven Microresonators," *Sensors and Materials,* v. 7, no. 6, pp. 415-430, 1995.

[66] G. K. Fedder, *Simulation of Microelectromechanical Systems*, Ph.D. Thesis, Dept. of Electrical Engineering and Computer Science, University of California at Berkeley, Sept. 1994.

[67] S. Iyer, *Layout Synthesis of Microresonators*, M.S. thesis, Carnegie Mellon University, May, 1998.

[68] P. E. Gill, W. Murray, M. A. Saunders and M. H. Wright, *User's Guide for NPSOL*, Systems Optimization Laboratory, Dept. of Operations Research, Stanford University, SOL 86-2, January 1986.

[69] B. Baidya, S. K. Gupta and T. Mukherjee, "Feature-recognition for MEMS Extraction," in *Proc. 1998 ASME Design Engineering Technical Conferences (DETC '98) - 25th Biennial Mechanisms Conference*, paper DETC98/MECH-5838, Atlanta, Sept. 1998.

[70] L. R. Carley, G. G. E. Gielen, R. A. Rutenbar and W. M. C Sansen, "Synthesis Tools for Mixed-Signal ICs: Progress on Frontend and Backend Strategies," in *Proc. of the IEEE/ACM Design Automation Conference*, June 1996, pp 298-303.

[71] IEEE 1076.1 Working Group, http://vhdl.org/vi/analog.
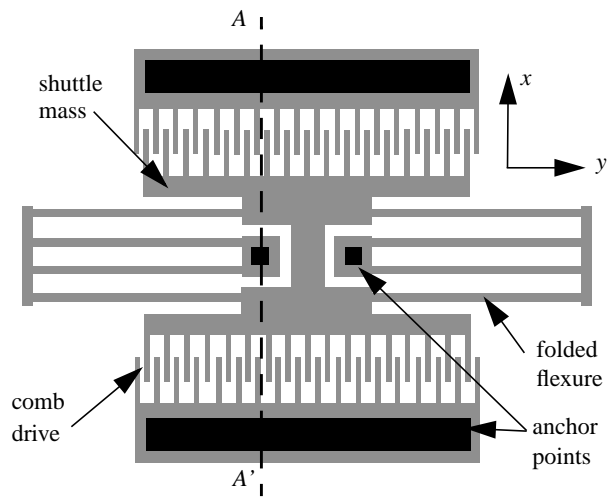
Figure 1: A folded-flexure comb-drive microresonator layout fabricated in a surface-micromachined polysilicon process.

(a)

2.0

PSG   dimple   photoresist

nitride   polysilicon

0.5

0.5

~ 500

n-type (100) silicon

(a)

(b)

structural polysilicon

2.0

(b)

(c)

(c)

(d)

released structure   anchor

(d)
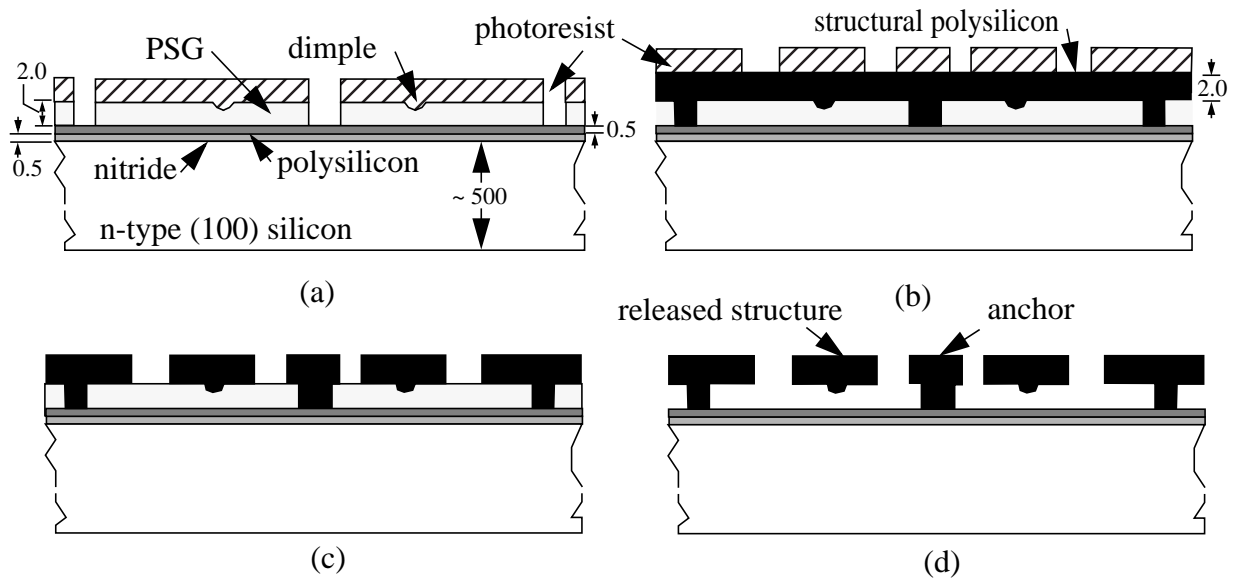
Figure 2: Polysilicon surface-micromachining process steps. (a) After sacrificial PSG deposition and patterning. (b) After deposition of structural polysilicon and patterning of photoresist. (c) After etching of structural polysilicon. (d) After the final release. All dimensions in microns.
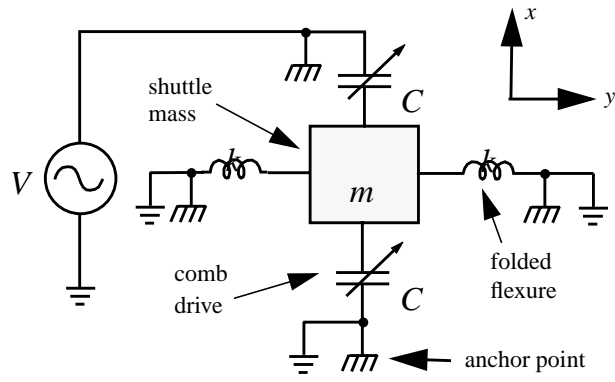
Figure 3: Mixed-domain schematic of the lateral folded-flexure comb-drive microresonator, including a voltage source, V, for comb-drive actuation.

folded-flexure resonator

comb drive

folded flexure

shuttle mass

anchor

beam

gap

plate

(a) (b) (c)
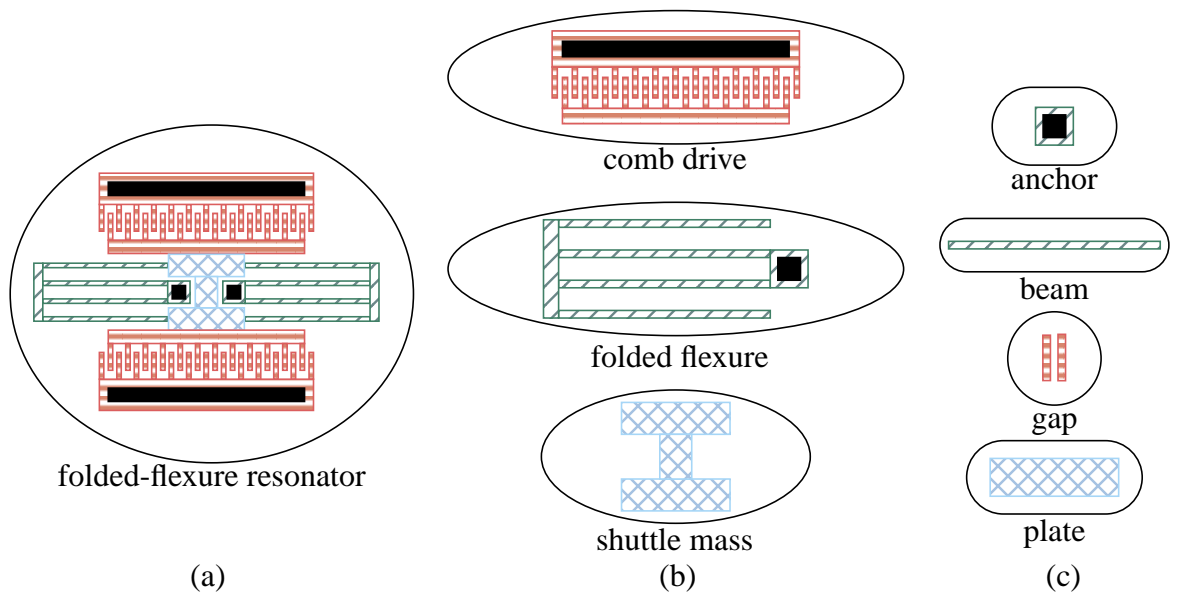
Figure 4: Decomposition of a folded-flexure resonator. (a) Resonator component. (b) Functional elements. (c) Atomic elements.
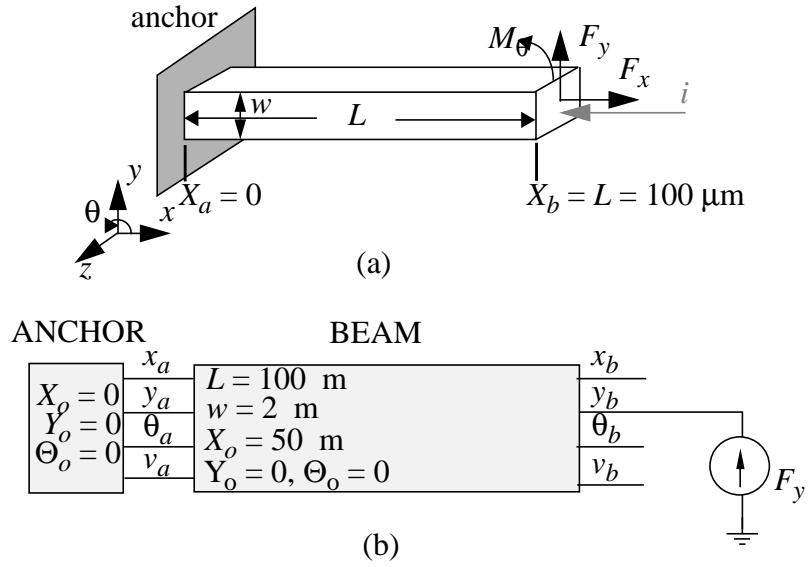
Figure 5: MEMS circuit representation of a simple cantilever beam with in-plane displacements (x, y, θ) and generalized forces (F_x, F_y, $M_θ$). (a) Physical view of the beam. (b) Behavioral schematic of the beam with a single force applied in the y direction. The values of y_b and $θ_b$ will increase as a result of the applied force.
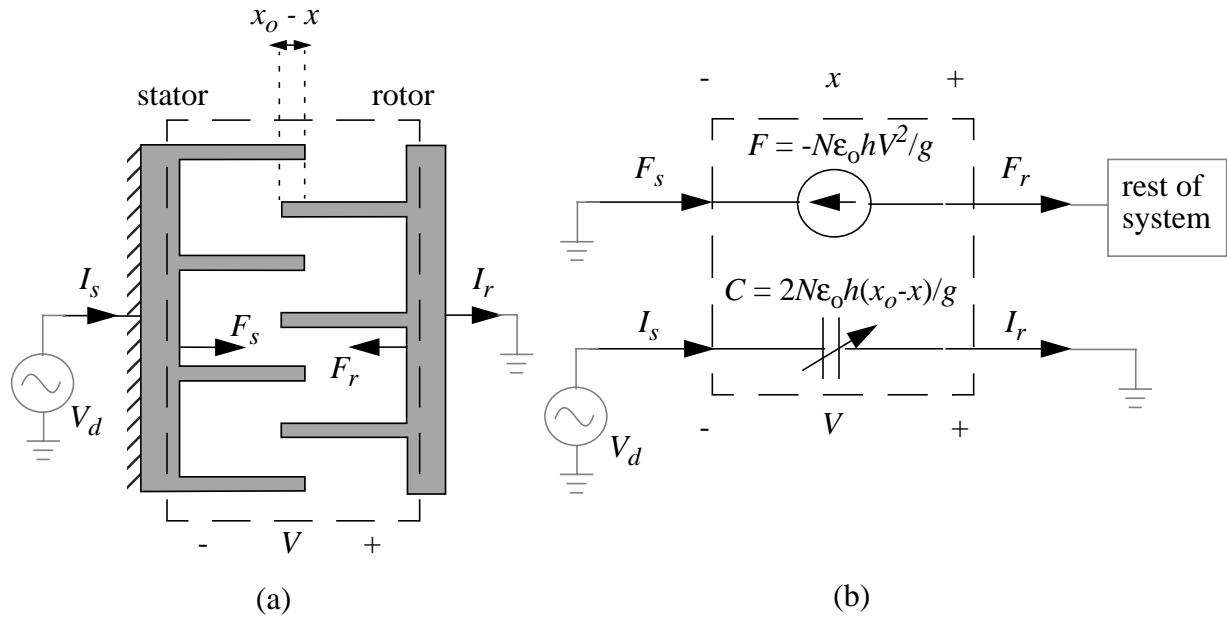
Figure 6: One-dimensional electromechanical model of the comb drive. (a) Layout showing the displacement current passing through the comb drive and the attractive electrostatic force. (b) The comb drive model with force as a dependent source and capacitance as a time-varying element.

ANCHOR

10k

transresistance
amplifier

COMB DRIVE-Y
finger_length: 40u
overlap: 20u
gap: 2u
finger_width: 2u
rotor_fingers: 80
angle:90

–
oab
+

gnd

PLATE MASS
N-S

l: 10u
w: 640u
angle:0

plate mass
elements

beam
elements

PLATE-MASS

Faces

l: 36u
w: 50u
angle:0

BEAM

L:177u
w:4u
angle:0

BEAM

L:177u
w: 4u
angle:0

L:34u
w:6u
angle:90

BEAM

L:34u
w:6u
angle:90

BEAM

ANCHOR

ANCHOR

BEAM

L:177u
w:4u
angle:0

BEAM

L:177u
w:4u
angle:0

L:34u
w:6u
angle:90

BEAM

PLATE MASS
N-S

l: 66u
w: 18u
angle:0

v
35.35

L:34u
w:6u
angle:90

BEAM

anchor
points

BEAM

L:177u
w: 4u
angle:0

ANCHOR

ANCHOR

BEAM

L:177u
w: 4u
angle:0

L:34u
w:6u
angle:90

BEAM

L:34u
w:6u
angle:90

BEAM

PLATE-MASS

Faces

l: 36u
w: 50u
angle:0

BEAM

L:177u
w:4u
angle:0

BEAM

L:177u
w:4u
angle:0

PLATE MASS
N-S

l: 10u
w: 640u
angle:0

electrostatic
actuator
element

COMB DRIVE-Y
finger_length: 40u
overlap: 20u
gap: 2u
finger_width: 2u
rotor_fingers: 80
angle:90

ANCHOR

vsine
ampl:35.35
f:30k

voltage
source

Figure 7: Mixed-domain schematic representation of a microresonator. Parameter values are listed next to each element symbol. A transresistance amplifier detects the displacement current generated by the motion of the resonator.

(a) displacement dB (m)

30350 Hz, -112.5 dB

f (kHz)

(b) displacement (µm)

2.5 µm

t (ms)
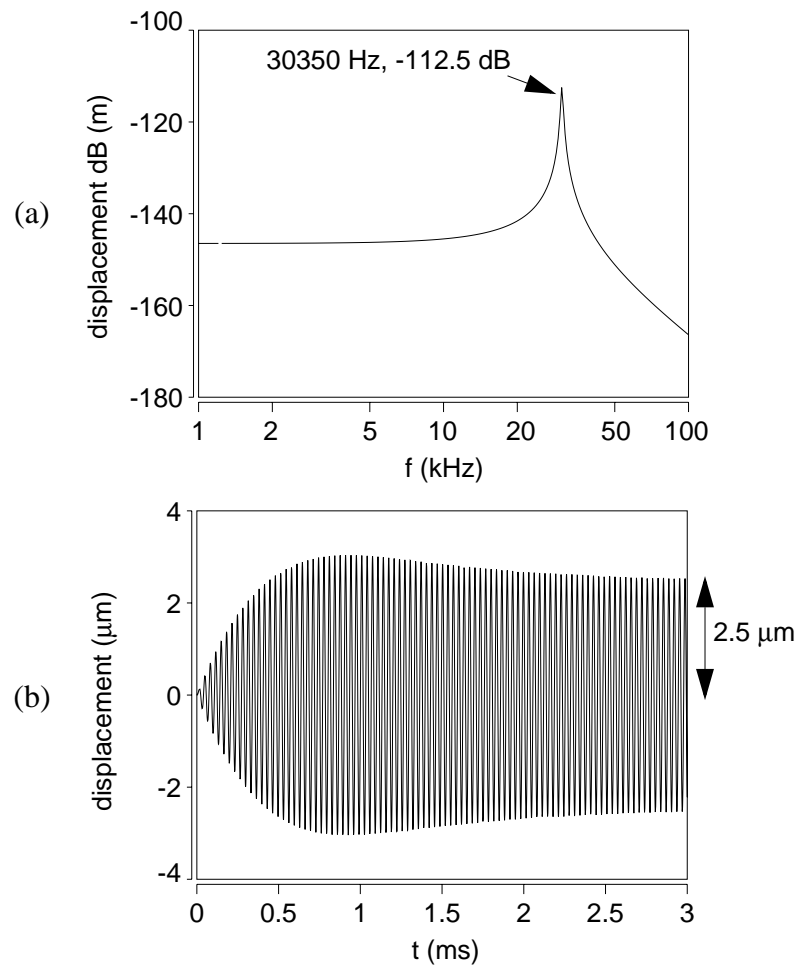
Figure 8: Microresonator circuit simulation results. (a) A.C. analysis (b) Transient analysis.
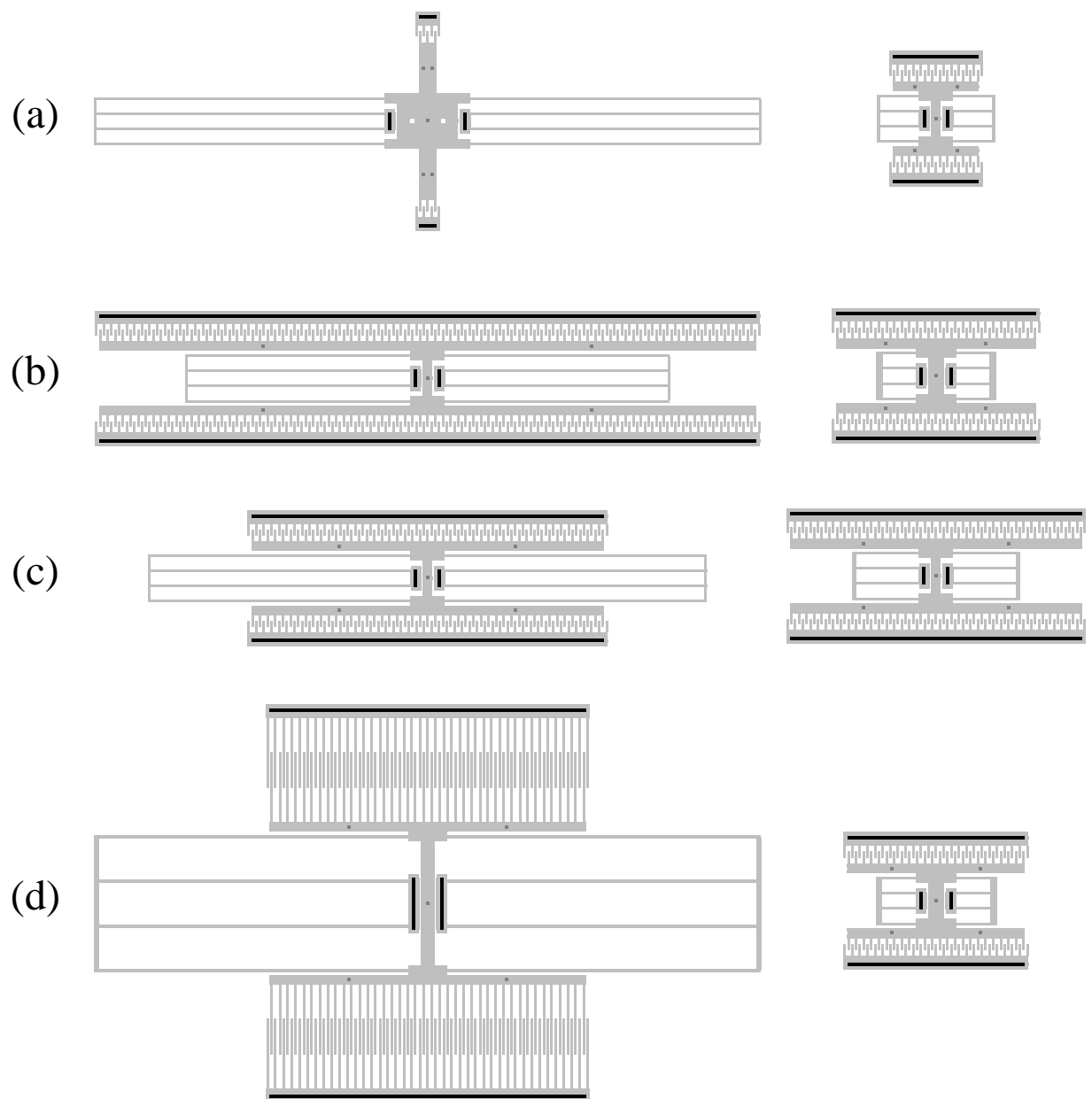
Figure 9: Resonators synthesized for four different design objectives: (a) minimize active area, (b) minimize drive voltage, (c) minimize combination of active area and drive voltage, and (d) maximize displacement. Resonant frequencies are 10 kHz (left) and 300 k(Hz) (right)
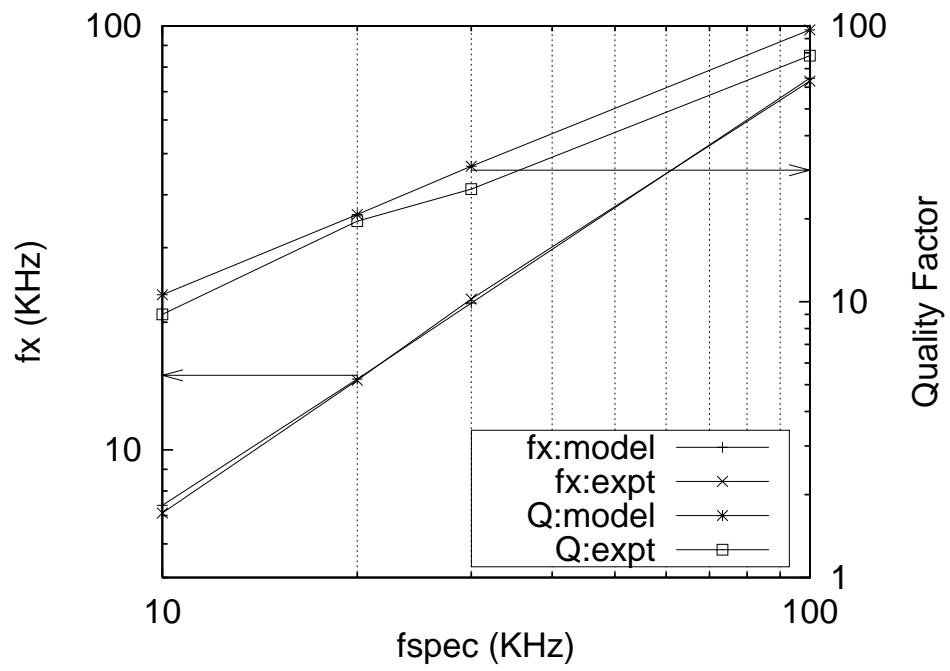
Figure 10: Comparison of measurements of resonant frequency and quality factor with analytical models.
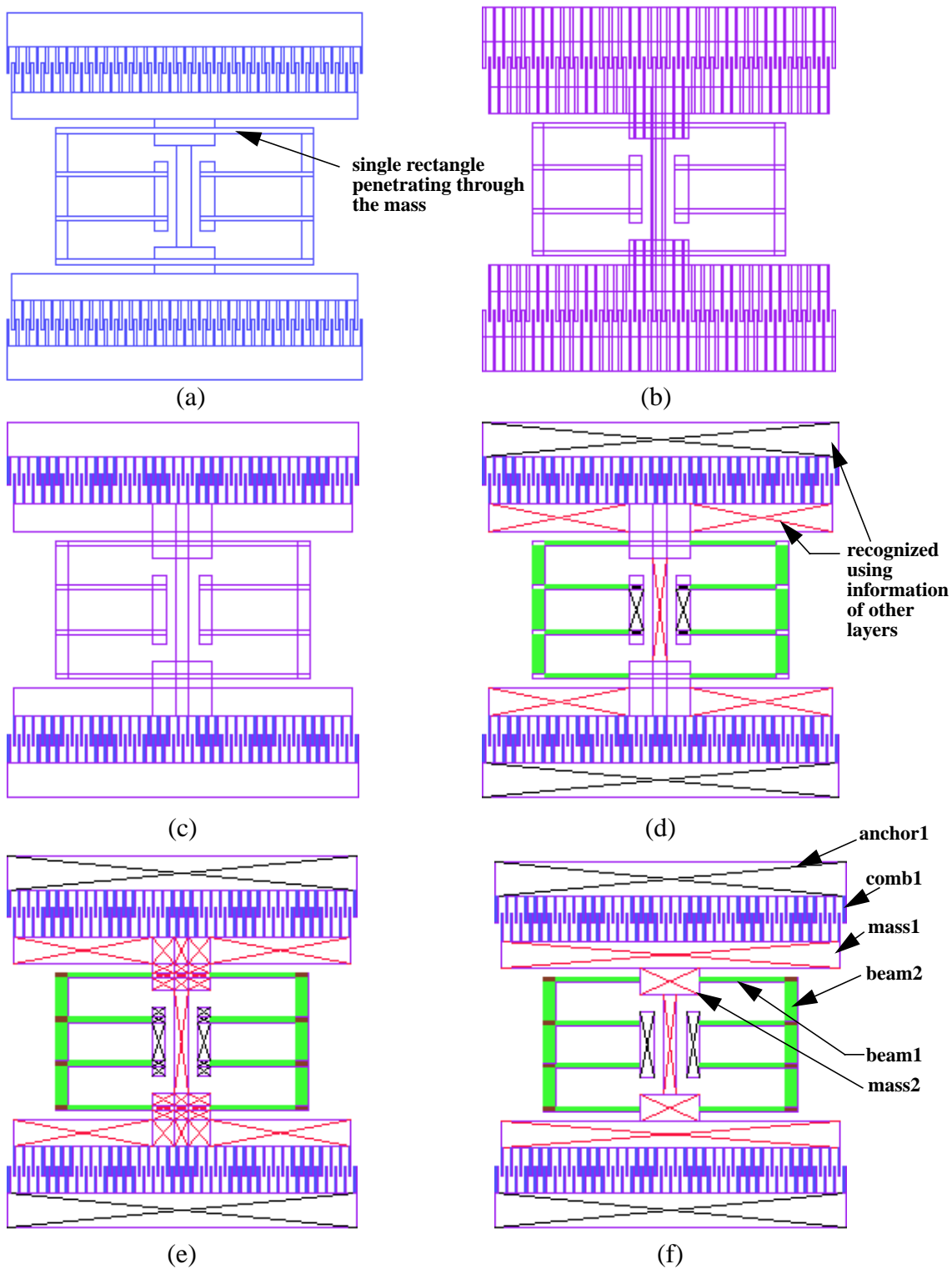
Figure 11: Folded-flexure resonator. (a) layout, (b) canonical representation, (c) canonical representation after separating the fingers, (d) intermediate state, (e) detected state, (f) optimized result. Each type of recognized element is shaded differently.

System Concept

System Architecture

System Simulation

Component Schematic

Component Synthesis

Component Simulation

Component Layout

System Layout

Component Extraction

System Extraction

Fabricate
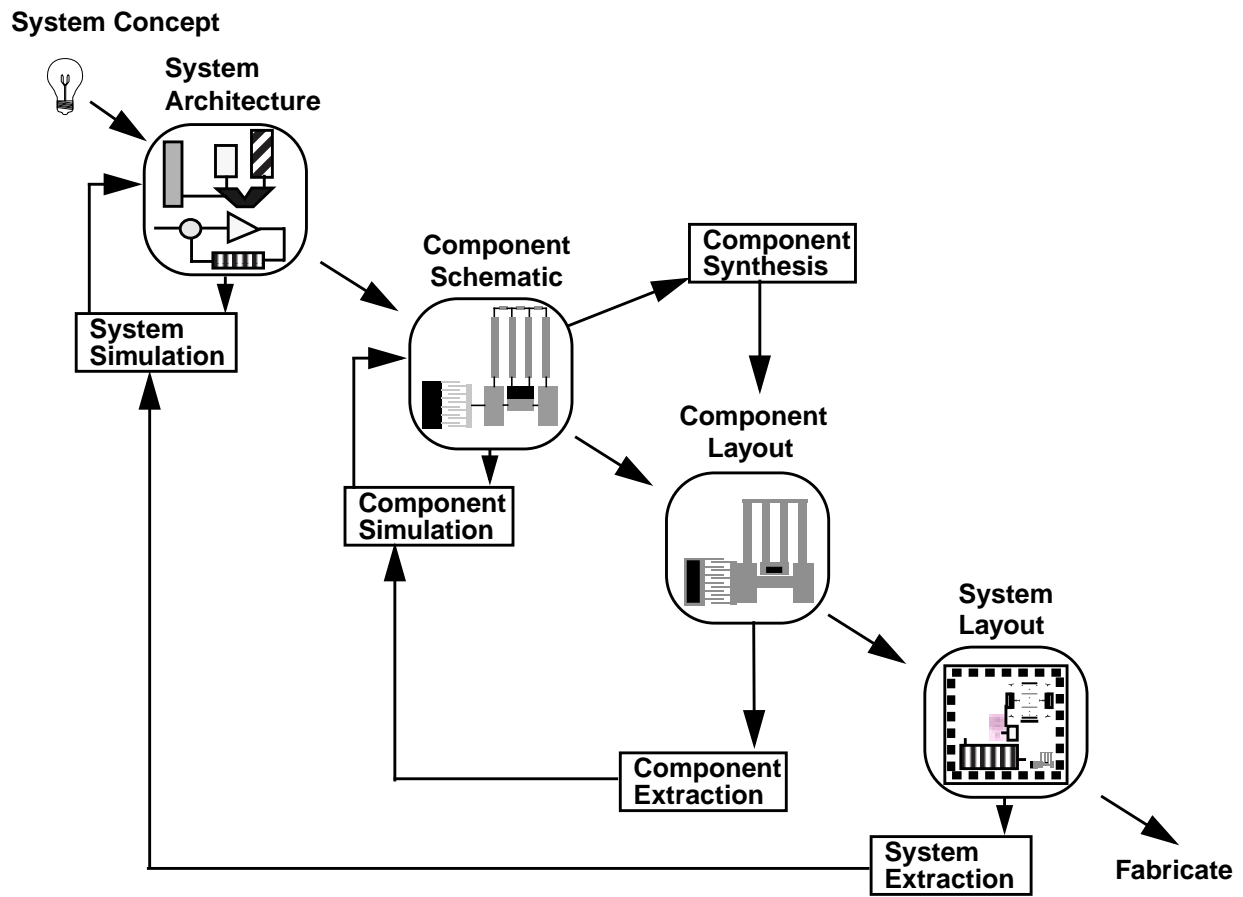
Figure 12: Mixed-domain design methodology.

11. Author Bio

Tamal Mukherjee is a Research Engineer and Assistant Director of the Center for Electronic Design Automation in Electrical and Computer Engineering Department at Carnegie Mellon University. He received his B.S., M.S. and Ph.D. degrees from Carnegie Mellon University in 1987, 1990, and 1995 respectively. His research interests include CAD tools to support analog circuit design and MEMS design, as well as numerical optimization algorithms.

Gary K. Fedder is an Associate Professor at Carnegie Mellon University holding a joint appointment with the Department of Electrical and Computer Engineering and The Robotics Institute. He received the B.S. and M.S. degrees in electrical engineering from MIT in 1982 and 1984, respectively. From 1984 to 1989, he worked at the Hewlett-Packard Company on circuit design and printed-circuit modeling. In 1994, he received the Ph.D. degree from U. C. Berkeley, where his research resulted in the first demonstration of multimode control of a underdamped surface-micromachined inertial device. He received the 1993 AIME Electronic Materials Society Ross Tucker Award, the 1996 Carnegie Institute of Technology G.T. Ladd Award, and the 1996 NSF CAREER Award. His present research interests include microsensor and microactuator design and modeling, integrated MEMS manufactured in CMOS processes, and structured design methodologies for MEMS.

CONSENT TO PUBLISH & TRANSFER OF COPYRIGHT

Under the United States Copyright Law, the transfer of copyright from the author should be explicitly stated in writing to enable the publisher to publish and disseminate the author's work to the fullest extent.

TITLE OF CONTRIBUTION: (please fill in)

Hierarchical Mixed-Domain Circuit Simulation, Synthesis and Extraction

Methodology for MEMS

AUTHOR(S): (please fill in)
Tamal Mukherjee

Gary K. Fedder

NAME OF JOURNAL:

JOURNAL OF VLSI SIGNAL PROCESSING SYSTEMS,
SPECIAL ISSUE ON SYSTEM DESIGN
EDITED BY ASIM SMAILAGIC

PART A - COPYRIGHT TRANSFER FORM AND WARRANTIES

2. In return for said rights, Publisher grants to Author the following rights.

 a.   All proprietary rights relating to the Article, other than copyright, such as patent rights.

 b.   The right to use, after publication, part or all of the Article in subsequent works of Author, provided that written permission is granted by Publisher, and that proper acknowledgement is made to the source and to the Publisher.

 c.   The right to make oral presentation of the material in any form.

 d.   In the case of work performed under United States Government contract, Publisher grants the U.S. Government royalty-free permission to reproduce all or portions of the Article and to authorize others to do so for U.S. Government purposes.

3. Any other use or reproduction of the work requires a fee and/or permission from Publisher.

4. In the event that the Article is not accepted and published by Publisher, this agreement becomes null and void.

5. Author warrants that the Article is original work and has not been published before in any form and that it does not infringe upon any copyright, contains no libelous or otherwise unlawful statements, and does not otherwise infringe on the rights of others, and that any necessary permission to quote from another source has been obtained. (In some journals, articles that have appeared in conference proceedings are acceptable; therefore, if this is the case, Author should annotate this agreement by including the date and name of the conference at the bottom.)

6. The Author declares that any person named as co-author of the Contribution is aware of the fact and has agreed to being so named.

                                                             March 10, 1999

_____
AUTHOR (and Title, if not author)   Date

PART B - U.S. GOVERNMENT EMPLOYEE CERTIFICATION

  Note: If your work was performed under Government contract,
        but you are not a Government employee, sign transfer
        form above and see Item 2d above.

This will certify that all authors of the above paper are employees of
the U.S. Government and performed this work as part of their
employment and that the paper is therefore not subject to U.S.
Copyright protection.

_____

AUTHORIZED SIGNATURE/TITLE   CONTRACT #

_____

NAME OF GOVERNMENT ORGANIZATION   DATE FORM SIGNED

Return form to:

      See address above

==
For Publisher's use only:

    Ms. Reference No. _____